The main conclusions to emerge from this study can be summarized as follows:

(*a*) All the distortion indices DI(PO), DI(OPO) and DI(OO) for the HPO_4 and H_2PO_4 types correlate with O···O and show an increase with increasing O···O. The magnitude and variation of DI(OO) is small compared with those of the DI(PO) and DI(OPO).

(*b*) The mean values of P–O, OPO and O–O are preserved for each H_nPO_4 group.

(*c*) The correlation is less clear in the H_2PO_4 than in the HPO_4 type, partly because the mutual configuration of the two hydrogen bonds affects the values of the geometrical parameters and obscures the correlations.

(*d*) The O···O dependence of the PO_4 distortion is approximately described by a model in which with increasing O···O the P atom moves in a direction away from the centroid of the regular tetrahedral framework of O atoms, while retaining $3m$ site symmetry for the HPO_4 type (Fig. 3*a*) and $mm2$ site symmetry for the H_2PO_4 type (Fig. 3*b*).

The author's thanks are due to the Kurata Research Grant for partial financial support and to the Ministry of Education, Science and Culture for a Grant-in-Aid for Scientific Research. The computations were performed on the HITAC M-280H of the Hokkaido University Computing Center.

References

BAUR, W. H. (1970). *Trans. Am. Crystallogr. Assoc.* **6**, 129-155.
BAUR, W. H. (1974). *Acta Cryst* B**30**, 1195-1215.
BAUR, W. H. (1981). *Structure and Bonding in Crystals*, edited by M. O'KEEFFE & A. NAVROTSKY, Vol. II, ch. 15. New York: Academic Press.
BAUR, W. H. & KHAN, A. A. (1970). *Acta Cryst.* B**26**, 1584-1596.
BROWN, I. D. (1981). *Structure and Bonding in Crystals*, edited by M. O'KEEFFE & A. NAVROTSKY, Vol. II, ch. 14. New York: Academic Press.
CATTI, M., FERRARIS, G. & IVALDI, G. (1979). *Acta Cryst.* B**35**, 525-529.
CRUICKSHANK, D. W. J. (1961). *J. Chem. Soc.* pp. 5486-5504.
DICKENS, B. & BOWEN, J. S. (1971). *Acta Cryst.* B**27**, 2247-2255.
DICKENS, B., PRINCE, E., SCHROEDER, L. W. & BROWN, W. E. (1973). *Acta Cryst.* B**29**, 2057-2070.
FERRARIS, G. & IVALDI, G. (1984). *Acta Cryst.* B**40**, 1-6.
GIBBS, G. V., MEAGHER, E. P., NEWTON, M. D. & SWANSON, D. K. (1981). *Structure and Bonding in Crystals*, edited by M. O'KEEFFE & A. NAVROTSKY, Vol. I, ch. 9. New York: Academic Press.
GILBERT, J. D. & LENHERT, P. G. (1978). *Acta Cryst.* B**34**, 3309-3312.
GILBERT, J. D., LENHERT, P. G. & WILSON, L. K. (1977). *Acta Cryst.* B**33**, 3533-3535.
ICHIKAWA, M. (1979*a*). *Acta Cryst.* B**35**, 1300-1301.
ICHIKAWA, M. (1979*b*). *J. Cryst. Mol. Struct.* **9**, 87-105.
JÖNSSON, P.-G. (1972). *Acta Chem. Scand.* **26**, 1599-1619.
LINES, M. E. & GLASS, A. M. (1977). *Principles and Applications of Ferroelectrics and Related Materials*. Oxford: Clarendon Press.
PAULING, L. (1960). *The Nature of the Chemical Bond*, 3rd ed., p. 547. Ithaca: Cornell Univ. Press.
PRELESNIK, B., HERAK, R., ČURIĆ, M. & KRSTANOVIĆ, I. (1978). *Acta Cryst.* B**34**, 76-78.
SAKURAI, T. (1967). Editor. *Universal Crystallographic Computing System*. The Crystallographic Society of Japan, Tokyo.
TAKAGI, S., MATHEW, M. & BROWN, W. E. (1980). *Acta Cryst.* B**36**, 766-771.
TOKUNAGA, M. & TATSUZAKI, I. (1984). *Phase Transitions*, **4**, 97-156.

Acta Cryst. (1987). B**43**, 28-34

A Structural Analysis of Potassium, Rubidium and Caesium Substitution in Barium Hollandite

BY ROBERT W. CHEARY

School of Physics and Materials, New South Wales Institute of Technology, PO Box 123, Broadway, New South Wales, Australia 2007

(*Received* 14 *April* 1986; *accepted* 10 *July* 1986)

Abstract

The changes in crystal structure of the barium hollandite $Ba_x(Al_{2x}Ti_{8-2x})O_{16}$ ($x = 1{\cdot}11$ and $1{\cdot}24$) with barium being partially substituted by K, Rb or Cs, have been determined using the Rietveld method on high-resolution neutron powder diffraction data. When K and Rb are substituted, solid solutions form with compositions conforming to a linear combination of the end members $Ba_{1{\cdot}24}(Al_{2{\cdot}48}Ti_{5{\cdot}52})O_{16}$ and $Rb_{1{\cdot}5}$ or $K_{1{\cdot}5}(Al_{1{\cdot}5}Ti_{6{\cdot}5})O_{16}$. Cs substitution however, is limited to approximately 0.25 Cs ions per unit cell for specimens prepared in air at atmospheric pressure. The compositions in this range can be described as a linear combination of the end members $Ba_{1{\cdot}11}(Al_{2{\cdot}22}Ti_{5{\cdot}78})O_{16}$ and $Cs_{1{\cdot}32}(Al_{1{\cdot}32}Ti_{6{\cdot}68})O_{16}$. This limit is imposed by the large size of Cs which prevents the ion occupying sites in the *c*-axis tunnels next to

0108-7681/87/010028-07$01.50

sites already occupied in ±c direction. In the known ordered structures of tunnel ions, the number of occupied sites containing unoccupied neighbours decreases as the total *A*-site occupancy increases. The limit of substitution given by calculation is 0·28 Cs ions per unit cell which agrees well with the observed limit. The preference of Cs for 'lone' sites is also manifested through the *c* parameter and the average volume of each tunnel site which only change by small amounts, compared with Rb- and K-substituted hollandites. In addition, the average off-centre shift of the Ba and Cs ions decreases, whereas in K- and Rb-substituted hollandites this remains substantially constant. The lateral expansion of the tunnels and the change in *a* is proportionately greater for the Cs-substituted hollandite.

Introduction

The synthetic rock SYNROC originally proposed by Ringwood (1978) is currently being tested as a host for radioactive waste. It consists of three major phases, perovskite, zirconolite and hollandite, each of which will accommodate a range of radwaste elements in solid solution. Barium hollandite, the subject of the present study, acts as a host for large alkali ions such as Cs and Rb. The general unit-cell formula of hollandites is $A_xB_8O_{16}$ ($x<2$) where *A* represents ions in the tunnel cavities (*e.g.* Ba, Cs, Rb or K) and *B* are smaller ions such as Mg, Ti or Al octahedrally coordinated by O. They are normally tetragonal [space group $I4/m$ with $a\approx 10$ and $c\approx 3$ Å (Sinclair, McLaughlin & Ringwood, 1980)] but when the ratio of the ionic radii R_A/R_B drops below approximately 2·08, the symmetry is often reduced to monoclinic [space group $I2/m$ with $\beta\approx 91°$ (Post, Von Dreele & Buseck, 1982; Cheary, 1986)]. The *A* ions frequently adopt an ordered arrangement along the *c*-axis tunnels (Bursill & Grzinic, 1980) with periodicities in the **c** direction which can be either commensurate or incommensurate with the hollandite lattice. Barium hollandites with 1·2 Ba ions per unit cell tend to form commensurate superstructures with 5*c* supercells, whereas those with 1·14 Ba ions per cell usually possess an incommensurate superstructure consisting of an intergrowth of 5*c* and 2*c* (or 4*c*) supercells (Pring, 1983; Kesson & White, 1986). Ordering shows up readily in electron diffraction patterns as superlattice reflections, but hardly at all in neutron or X-ray powder diffraction patterns.

In SYNROC compositions, the host hollandites range between $Ba_x(Al_{2x}Ti_{8-2x})O_{16}$ ($x=1{\cdot}14$ or $x=1{\cdot}23$) and $BaTi_8O_{16}$ (Kesson & White, 1986). With radwaste ions substituted into the tunnels, the general unit-cell formula is

$$Ba_xM_y[(Al^{3+}Ti^{3+})_{2x+y}Ti_{8-2x-y}]O_{16}$$

where *M* is the substituted ion (*i.e.* Cs, Rb or K). Both K and Rb can completely replace Ba and fully occupy the tunnel cavities (Bayer & Hoffmann, 1966). At atmospheric pressure and under oxidizing conditions, approximately 20% of the Ba can be replaced by Cs in hollandites containing no Ti^{3+} ions (Roth, 1981; Cheary & Kwiatkowska, 1984). Cs only substitutes in high concentrations when the preparation is carried out at high pressure in a reducing environment. Under these conditions, Kesson & White (1986) have prepared hollandites with Cs only at the tunnel sites (*e.g.* $Cs_{1\cdot32}Ti_8O_{16}$).

The purpose of the present work is to examine the way in which the crystal structure of barium hollandite changes when K, Rb and Cs are incorporated into the tunnel cavities. Although Cheary & Kwiatkowska (1984) have previously examined Cs substitution by X-ray powder diffraction, their work is repeated here to some extent because of inconsistencies in their site occupancies and the presence of preferred orientation in their diffraction samples.

The crystal structure of barium hollandites

The structure of barium hollandite is shown in Fig. 1. The Ba atoms in the tunnels are normally located off-centre in the **c** direction either above or below the centre of a box of eight coordinating O ions. The choice of off-centre position is determined principally by the local electrostatic field set up between neighbouring occupied sites. Each tunnel is bounded by four walls of edge-sharing octahedra with the octahedra at the hinges between the walls sharing a common corner [*i.e.* O2(1′), O2(2′), O2(3′) and

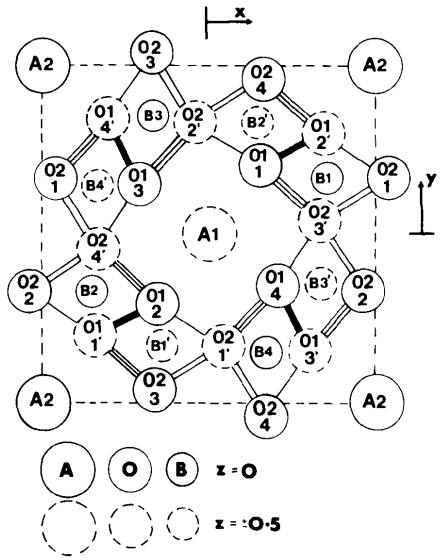

Fig. 1. Projection of the hollandite structure onto the (001) plane showing the atomic positions generated by the $I4/m$ space group. O–O bonds depicted with similar line patterns have the same bond length.

O2(4')]. In tetragonal hollandites, all the octahedra are identical, but are distorted by the off-centre shift of the octahedral cations. This shift arises from the electrostatic repulsion between each column of octahedral cations within the walls and results in a shortening of the common edge O–O bond [*e.g.* O1(1)–O1(2')] and an elongation of the O–O bond associated with O ions in contact with the octahedral ion [*e.g.* O2(1)–O2(3')].

Specimen preparation

Although K- and Rb-substituted hollandites are relatively easy to prepare by solid-state reaction of the component oxides and carbonates (Bayer & Hoffmann, 1966), some allowance has to be made for the loss of K or Rb by volatilization during the final firing. When a hollandite is prepared from a mixture of starting materials corresponding to a composition in the solid-solution range between $Ba_{1\cdot23}(Al_{2\cdot46}Ti_{5\cdot54})O_{16}$ and $M_2(Al_2Ti_6)O_{16}$ (M = Rb or K), the X-ray powder pattern of the product normally contains weak second-phase lines due to Al_2O_3 as a result of the loss of K_2O or Rb_2O during firing. The hollandite formed therefore contains a smaller than expected proportion of K or Rb. In the present work, the starting mixture required for each specimen was determined as part of a preliminary investigation in which the proportion of Al_2O_3 in a range of starting mixtures was gradually reduced until no trace of this component could be observed in the X-ray pattern of the fired product. The same approach was adopted to determine the optimum starting mixtures for preparing Cs-substituted hollandites, as Cs_2O also volatilizes during firing (Kesson, 1983). However, at concentrations estimated by XRF to be greater than approximately 0·25 Cs ions per unit cell, diffraction lines other than those of Al_2O_3 or hollandite appear in the X-ray patterns. Also, the composition of the hollandite phase formed at these higher concentration levels remains the same and is independent of the Cs concentration in the starting mixture. Up to approximately 0·25 Cs ions per cell, the specimens are single-phase hollandites and the lattice parameters increase with increasing Cs concentration. Beyond this level, the specimens are multiphase and the lattice parameters do not change significantly. Clearly, once the saturation concentration of Cs in hollandite is exceeded, any additional Cs either volatilizes or is used to form the impurity phase. This behaviour has also been noted by Roth (1981) who found that for specimens prepared in air, only about 20 mole percent of Ba could be replaced by Cs and that additional Cs resulted in the formation of a Cs mixed-metal oxide which has recently been identified as $Cs_2Al_2Ti_2O_8$ (Solomah & Odoj, 1984). Hollandite specimens with higher concentrations of Cs can be prepared, but only under hot-pressing conditions (Roth, 1981; Kesson, 1983; Kesson & White, 1986).

In the present work, all the hollandites were made up from mixtures of TiO_2, Al_2O_3, $BaCO_3$ and either K_2CO_3, Rb_2CO_3 or Cs_2CO_3. The Rb- and K-substituted hollandite specimens were prepared with approximately 0·45 and 0·85 substituted ions per unit cell; the Cs-substituted specimen was prepared with approximately 0·2 Cs ions per unit cell (*i.e.* close to the saturation composition). To do this, each starting mixture was wet ground in acetone, cold pressed into a 25 mm disc and then calcined in air at 1080 K for 4 h. After further wet grinding, each specimen was again cold pressed into a disc and fired in air at temperatures between 1570 and 1640 K for 8–10 h. X-ray diffraction scans of all the specimens revealed well-crystallized single-phase tetragonal hollandites.

Measurement and refinement procedures

Neutron diffraction data were collected for each of the specimens using the eight-detector high-resolution powder diffractometer at the Australian Atomic Energy Commission Research Laboratories (Howard, Ball, Davis & Elcombe, 1983) with an incident wavelength of 1·377 Å. All the measurements were carried out at room temperature (296–298 K) with finely ground specimens compacted into a thin-walled vanadium can mounted on the rotating stage of the diffractometer. Each set of count data was recorded at fixed monitor counts over an angular range $2\theta = 0$–$150°$ in steps of $0{\cdot}05°$ 2θ.

The structural parameters were refined from the neutron data by the Rietveld method (Rietveld, 1969) using the program developed by Wiles & Young (1981) and implemented at the Australian Atomic Energy Commision by Drs C. J. Howard and R. J. Hill. In the refinement, the diffraction profiles were fitted by a sum of Gaussians to allow for profile asymmetry (Howard, 1982) whilst the background was fitted to a polynomial of the form $\sum a_i x^i$ where $i = -1$ to $+2$ and $x = 2\theta$. The goodness-of-fit indicators quoted in the table of refined structural parameters (Table 1) are the weighted-pattern R factor R_{wp}, its expected value R_{wp}^E based on the neutron count statistics, and the Bragg R factor R_B.

In the refinement, the Ba and substituted ions (K, Rb or Cs) were assumed to be randomly distributed over the tunnel A sites. Similarly, the Al and Ti ions were assumed to be randomly distributed over the octahedral B sites. Constraints were placed on the occupancies of the A and B sites to maintain charge neutrality over the unit cell and a total of eight Al + Ti ions at the B sites. Once stable instrumental, lattice and positional parameters had been obtained, anisotropic thermal parameters were introduced into the refinement. In general, the refinements converged rapidly and good fits were obtained for all the diffrac-

Table 1. *Structural parameters, unit-cell compositions, anisotropic thermal parameters β_{ij} and lattice parameters obtained by Rietveld refinement of the neutron powder diffraction data from* Ba *hollandites with* K, Rb *and* Cs *substituted in the tunnel sites*

	Barium hollandite 1	Barium hollandite 2	K-Ba hollandite 1	K-Ba hollandite 2	Rb-Ba hollandite 1	Rb-Ba hollandite 2	Cs-Ba hollandite
Ba/cell	1·109 (16)	1·242 (21)	0·835 (33)	0·440 (32)	0·837 (23)	0·443 (32)	0·965 (18)
K/cell	—	—	0·432 (33)	0·952 (32)	—	—	—
Rb/cell	—	—	—	—	0·480 (23)	0·909 (32)	—
Cs/cell	—	—	—	—	—	—	0·187 (18)
A-site total	1·109 (16)	1·242 (21)	1·267 (47)	1·392 (45)	1·317 (33)	1·352 (45)	1·152 (25)
z	0·407 (4)	0·362 (4)	0·381 (6)	0·371 (11)	0·375 (4)	0·373 (5)	0·424 (7)
$\beta_{11} = \beta_{22}$	0·0028 (6)	0·0023 (7)	0·0025 (8)	0·0041 (15)	0·0026 (6)	0·0048 (11)	0·0044 (9)
β_{33}	0·089 (28)	0·030 (10)	0·160 (37)	0·219 (74)	0·107 (18)	0·097 (18)	0·123 (38)
Ti/cell	5·784 (32)	5·515 (42)	5·898 (48)	6·166 (53)	5·850 (32)	6·205 (51)	5·885 (34)
Al/cell	2·216 (32)	2·485 (42)	2·102 (48)	1·834 (53)	2·150 (32)	1·795 (51)	2·115 (34)
x	0·3545 (6)	0·3525 (9)	0·3543 (7)	0·3512 (9)	0·3541 (6)	0·3516 (10)	0·3542 (7)
y	0·1692 (7)	0·1652 (11)	0·1686 (9)	0·1678 (11)	0·1662 (8)	0·1673 (12)	0·1680 (9)
β_{11}	0·0032 (5)	0·0041 (8)	0·0034 (6)	0·0022 (7)	0·0022 (5)	0·0023 (7)	0·0030 (6)
β_{22}	0·0049 (5)	0·0034 (7)	0·0048 (6)	0·0037 (7)	0·0041 (5)	0·0041 (7)	0·0039 (6)
β_{33}	0·016 (4)	0·019 (7)	0·021 (6)	0·024 (6)	0·011 (5)	0·016 (7)	0·0088 (40)
β_{12}	0·0012 (5)	0·0010 (10)	0·0022 (6)	−0·0010 (8)	0·0002 (6)	0·0002 (9)	0·0009 (6)
Oxygen x_1	0·1544 (2)	0·1545 (3)	0·1545 (3)	0·1545 (6)	0·1546 (3)	0·1543 (6)	0·1542 (3)
Oxygen y_1	0·2018 (2)	0·2011 (2)	0·2023 (2)	0·2037 (4)	0·2034 (2)	0·2044 (4)	0·2022 (3)
β_{11}	0·0017 (2)	0·0017 (2)	0·0020 (2)	0·0025 (3)	0·0020 (2)	0·0024 (4)	0·0015 (2)
β_{22}	0·0016 (2)	0·0013 (2)	0·0017 (2)	0·0017 (3)	0·0015 (2)	0·0013 (3)	0·0015 (2)
β_{33}	0·0060 (13)	0·0086 (17)	0·0099 (18)	0·011 (3)	0·0077 (15)	0·0072 (24)	0·0075 (18)
β_{12}	0·0002 (1)	0·0006 (2)	0·0003 (2)	0·0009 (3)	0·0002 (2)	0·0012 (4)	0·0005 (2)
Oxygen x_2	0·5414 (2)	0·5413 (3)	0·5414 (3)	0·5407 (4)	0·5408 (2)	0·5403 (4)	0·5417 (3)
Oxygen y_2	0·1656 (3)	0·1654 (4)	0·1653 (4)	0·1656 (5)	0·1661 (3)	0·1654 (6)	0·1650 (4)
β_{11}	0·0012 (1)	0·0010 (2)	0·0012 (2)	0·0009 (3)	0·0014 (2)	0·0016 (3)	0·0020 (2)
β_{22}	0·0027 (2)	0·0030 (3)	0·0027 (3)	0·0028 (4)	0·0022 (2)	0·0032 (4)	0·0030 (3)
β_{33}	0·0067 (12)	0·0065 (15)	0·013 (2)	0·0092 (24)	0·0093 (15)	0·0099 (25)	0·0088 (18)
β_{12}	−0.0001 (2)	−0·0002 (2)	0·0000 (2)	−0·0006 (4)	0·0001 (2)	−0·0008 (4)	0·0002 (2)
a (Å)	9·9750 (1)	9·9483 (2)	9·9877 (3)	10·0183 (3)	9·9988 (2)	10·0449 (4)	10·0004 (2)
c (Å)	2·92538 (4)	2·92421 (7)	2·92900 (8)	2·93348 (9)	2·92824 (6)	2·9330 (1)	2·92591 (7)
Goodness of fit (%)							
R_{wp}	5·9	8·1	6·3	8·1	5·9	5·7	5·8
R_E^{wp}	4·6	4·9	5·1	5·7	4·9	4·4	5·1
R_B	2·1	1·7	1·2	1·7	1·2	1·6	1·2

tion patterns with R_{wp} values ranging from 5·7 to 8·1% and Bragg R factors from 1·2 to 2·1%. Also, the refined occupancies agreed very well with the expected unit-cell compositions. The structural data obtained from the Rietveld refinement are presented in Table 1 along with structural data for the end-member Ba hollandites (Cheary, 1986). There are slight differences between these results and the earlier ones because the present refinements include anisotropic temperature factors.

Discussion

The refined structural parameters of the substituted hollandites are not radically different from those of the two Ba hollandites $Ba_{1\cdot11}(Al_{2\cdot22}Ti_{5\cdot78})O_{16}$ and $Ba_{1\cdot24}(Al_{2\cdot48}Ti_{5\cdot52})O_{16}$, denoted as the Ba(1·11) and Ba(1·24) hollandites, respectively. In Fig. 2, both the Rb- and K-substituted hollandites seem to be based on solid solutions having the Ba(1·24) hollandite as one end member. The compositions given by extrapolating the K and Rb data to the other end of the solid-solution range are similar and correspond to hollandites with between 1·45 and 1·50 K or Rb ions per cell. Potassium hollandites close to this composition range have previously been prepared by Beyeler (1976) and Weber & Schulz (1983). On the other hand, the Cs-substituted hollandite seems to be based on a linear combination of the Ba(1·11) hollandite and a pure Cs hollandite $Cs_x(Al_xTi_{8-x})O_{16}$ with x between 1·30 and 1·35. A pure Cs hollandite within this occupancy range [*i.e.* $Cs_{1\cdot32}(Ti^{3+}Ti^{4+})O_{16}$] has been prepared by Kesson & White (1986), but only by hot pressing in a reducing environment.

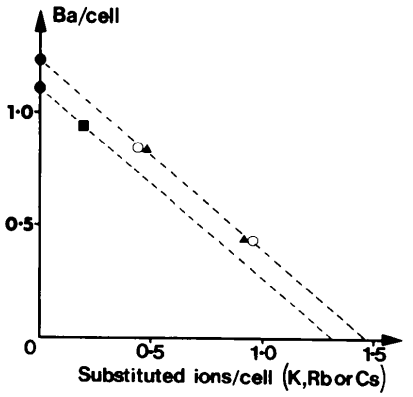

Fig. 2. Refined Ba occupancy plotted against the occupancy of each of the substituted ions K, Rb and Cs. In this graph ● correspond to the unsubstituted Ba hollandites, ○ to K substitution, ▲ to Rb substitution and ■ to Cs substitution.

The adoption of the Ba(1·11) hollandite and not the Ba(1·24) hollandite as the end member for the Cs-substituted hollandite is probably related to the large size of the Cs ion. In first place, the Ba(1·11) compound possesses a larger unit-cell volume and a larger *A*-site cavity volume than the Ba(1·24) hollandite (Cheary, 1986), and is therefore better able to accommodate this ion. More important, the ordered structure in the Ba(1·11) hollandite contains a larger number of occupied sites bounded by unoccupied adjacent sites in the $\pm c$ directions (hereinafter referred to as lone sites). In the various ordered structures proposed by Bursill & Grzinic (1980) with *A*-site occupancies between 0·8 and 1·33 ions per cell, the Ba ions occur either as pairs, with adjacent unoccupied sites, or as lone sites. This is illustrated in Fig. 3 which shows the ordered structures in hollandites with 0·8, 1·2 and 1·33 *A*-site ions per cell. The importance of the ordered structure is related to the fact that the *A*-site cavity in Ba hollandites is not large enough to accommodate Cs without considerable deformation of the surrounding structure. The distance between the centre of an *A* site and its eight surrounding O ions is approximately 2·92 Å in Ba hollandite, whereas the average Cs–O bond length is about 3·12 Å (Shannon, 1976). Cs-ion substitution will only be stabilized if the deformation can be absorbed by the surrounding structure. In the hollandite structure, this condition is satisfied if the Cs ions occupy lone *A* sites rather than sites next to a Ba ion or another Cs ion. In this way, the deformation along the tunnels is absorbed by the unoccupied adjacent cavities. In the K- and Rb-substituted hollandites this problem will be less pronounced as the Rb–O bond length (2·98 Å) is only slightly greater than the tunnel-cavity size, whereas the K–O bond length (2·89 Å) is less than the cavity size.

Any lateral deformation caused by a substituted ion can only be absorbed by expansion of the tunnel walls. The different extents to which K, Rb and Cs ions affect the lateral dimensions of the tunnels (*i.e.* perpendicular to *c*) is reflected in the plots of the average octahedral Ti/Al–O bond length and the width of the tunnel wall [*i.e.* O2(2′)–O2(3′) separation] as a function of the Ti/Al occupancy ratio (Figs. 4*a* and 4*b*). The width of the tunnel wall in the Cs-substituted hollandite lies above the trend of the other hollandites because of the additional stretching over and above the value set by the Ti and Al ions (Cheary, 1986). As a consequence of the lateral stretching, the average Ti/Al–O bond length on the octahedral sites is no longer just a function of the Ti/Al ratio at the octahedral sites. At a fixed Ti/Al ratio the average Ti/Al–O bond length increases slightly with the size of the substituted tunnel ion. The K-substituted hollandites follow a trend which is almost continuous with the Ba hollandites, whereas the Rb hollandites and the Cs hollandite have progressively larger Ti/Al–O bond lengths. The extra stretching of these bonds in Cs-substituted hollandites may introduce some degree of instability in the structure although this can be relieved to some extent by incorporating larger ions on the octahedral sites.

The experimental limit of approximately 0·25 Cs ions per cell for specimens prepared in air is probably determined by the number of available lone sites in the tunnels rather than by the tunnel-wall stretching. In the commensurate superstructures shown in Fig. 3, the number of lone sites per cell (q) is linearly related to the total *A*-site occupancy (z). If this relationship is assumed to be continuous over the range $z = 0{\cdot}8$–$1{\cdot}33$, then the average number of lone sites per cell in an incommensurate superstructure between these limits will be given by

$$q = 2{\cdot}00 - 1{\cdot}50z. \qquad (1)$$

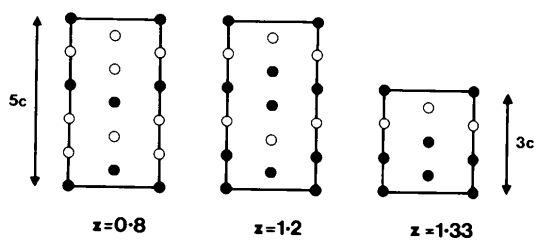

Fig. 3. (100) projections of the commensurate superstructures of the tunnel ions at occupancy levels z of 0·8, 1·2 and 1·33 ions per hollandite unit cell.

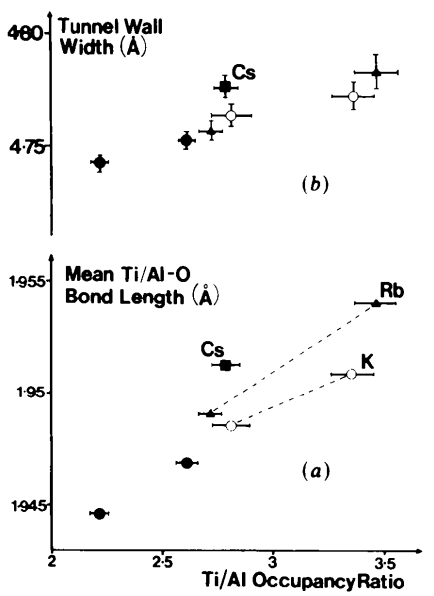

Fig. 4. Plots of (*a*) the mean Ti/Al–O bond length at the octahedral sites and (*b*) the wall width represented by the O2(2′)–O2(3′) separation against the ratio of the Ti/Al occupancies on the octahedral sites. In these plots ● correspond to the unsubstituted Ba hollandites, ○ to K substitution, ▲ to Rb substitution and ■ to Cs substitution.

Furthermore, if the allowed compositions of Cs-substituted hollandites can be represented as a linear combination of $Ba_{1\cdot10}(Al_{2\cdot20}Ti_{5\cdot80})O_{16}$ and an aluminous Cs hollandite within the range indicated in Fig. 2 [*viz.* $Cs_x(Al_xTi_{8-x})O_{16}$ with $1\cdot30 < x < 1\cdot35$], then the average number of Cs ions per cell (y) in such a hollandite [*viz.* $Cs_yBa_{z-y}(Al_{2z-y}Ti_{8-2z+y})O_{16}$] will be related to the occupancy z by the equation,

$$y = (z - 1\cdot10)/(0\cdot170 \pm 0\cdot015). \qquad (2)$$

The point at which the Cs occupancy exceeds the number of lone sites q corresponds to a composition with a total A-site occupancy of 1·15 ions per cell and a Cs occupancy of $0\cdot28 \pm 0\cdot01$ ions per cell. This occupancy level is comparable with the observed upper limit of approximately 0·25 Cs ions per cell.

The proposed partitioning of the Cs ions onto lone sites shows up in a number of structural properties. In particular, when the unit-cell volume or the A-site cavity volume expressed as a fraction of the unit-cell volume is plotted against the average Ti/Al-O bond length (Figs. 5*a* and 5*b*), the Ba, K and Rb hollandites all lie more or less on the same straight line. However, the results for the Cs-substituted hollandite are both depressed relative to the other hollandites, and the fractional A-site cavity volume of the Cs hollandite is almost identical to that of the end member Ba(1·11) hollandite. These effects arise because the partitioning of the Cs ions produces very little change in the c parameter. At a fixed Ti/Al occupancy, the c parameter is larger when the substituted A ions occupy paired sites, as must be the case in the K- and Rb-substituted hollandites. This is evident when the lattice parameters a and c of the hollandites are plotted against each other (see Fig. 6). Cs ions produce a large change in a and a comparatively small change in c, whereas the smaller Rb and K ions produce a large increase in c and a smaller change in a.

The pairing of K (or Rb) ions with other K or Ba ions also influences the average off-centre shift of these ions in the O cavities. In all the K- and Rb-substituted hollandites, the average off-centre shift is approximately 0·37(3) Å and not markedly different from the shift in the Ba(1·24) hollandite [0·40(1) Å]. On the basis of ionic size alone, the average off-centre shift should decrease as K or Rb ions are substituted for Ba ions. However, the total occupancy at the A sites for the K and Rb hollandites is close to the commensurate superlattice structure with $x = 1\cdot33$ ions, where all the A ions are paired (see Fig. 3) and experiencing mutual off-centring electrostatic forces. The fact that the average shift remains substantially constant is an indication of the strength of these forces. The behaviour of the Cs-substituted hollandite is quite different to the other substituted hollandites. With the addition of only 0·19 Cs ions per cell, the average off-centre shift drops from 0·27(1) Å in the Ba(1·11) hollandite to 0·22(2) Å. This again is consistent with the Cs ions occupying central positions in lone sites and the Ba ions occupying off-centre positions in paired sites.

The off-centre shifts given by refinement represent averaged values. For the substituted specimens, there will be a distribution of off-centre shifts which will depend on whether or not a lone site is occupied by a Ba or a substituted ion, and whether or not paired sites are occupied by similar or different ions (*e.g.*

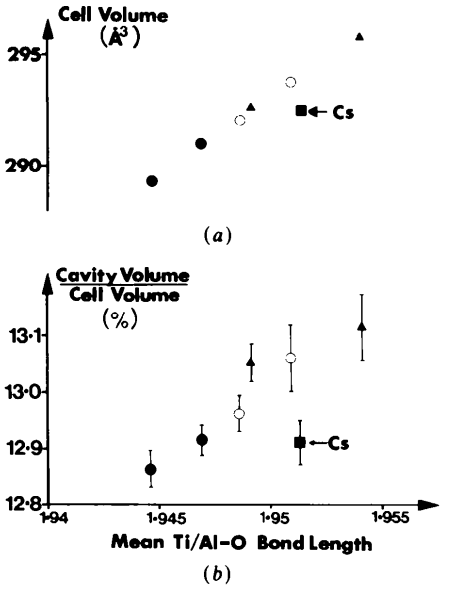

Fig. 5. Plots of (*a*) the unit-cell volume and (*b*) the tunnel-cavity volume expressed as a percentage of the unit-cell volume (*i.e.* $x_1^2 + y_1^2$) against the mean Ti/Al-O bond length. In these plots ● correspond to the unsubstituted Ba hollandites, ○ to K substitution, ▲ to Rb substitution and ■ to Cs substitution.

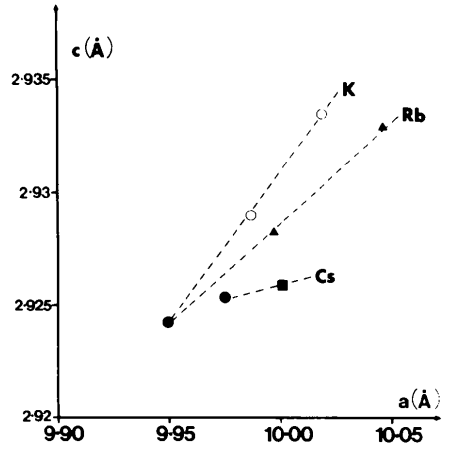

Fig. 6. The relationship between the lattice parameters a and c for the refined hollandites. In this graph ● correspond to the unsubstituted Ba hollandites, ○ to K substitution, ▲ to Rb substitution and ■ to Cs substitution.

Ba-Ba, K-K or Ba-K). In the present results and in the earlier work of Sabine & Hewat (1982), this shows up as an RMS static displacement contribution to the β_{33} anisotropic thermal parameters. In all the substituted hollandites, the apparent RMS amplitude of vibration U_{33} along the tunnels [given by $(\beta_{33}c^2/2\pi^2)^{1/2}$] is between two and three times the RMS amplitude U_{11} or U_{22} [given by $(\beta_{11}c^2/2\pi^2)^{1/2}$] perpendicular to the tunnel axis. In the Ba(1·24) hollandite, $U_{11} \simeq U_{33}$ and U_{11} is comparable with the values in the substituted specimens. On the assumption that the thermal vibrations are approximately isotropic and the U_{11} values are predominantly thermal in nature, an estimate of the RMS static displacement U_s will be given by $U_{33}^2 = U_{11}^2 + U_s^2$. Interpreted in this way individual off-centre shifts in the K and Rb hollandites can be anywhere between 0·15 and 0·65 Å. In the Cs-substituted hollandite the shifts are between 0·10 and 0·40 Å. The extent to which positional disorder contributes to U_{33} and U_{11} is currently under investigation.

I wish to acknowledge the support given to this work by the Australian Atomic Energy Commission (Research Contract No. 82/X/1) and the Australian Institute of Nuclear Science & Engineering.

References

BAYER, G. & HOFFMANN, W. (1966). *Am. Mineral.* **51**, 511-516.
BEYELER, H. U. (1976). *Phys. Rev. Lett.* **37**, 1557-1560.
BURSILL, L. A. & GRZINIC, G. (1980). *Acta Cryst.* B**36**, 2902-2913.
CHEARY, R. W. (1986). *Acta Cryst.* B**42**, 229-236.
CHEARY, R. W. & KWIATKOWSKA, J. (1984). *J. Nucl. Mater.* **125**, 236-243.
HOWARD, C. J. (1982). *J. Appl. Cryst.* **15**, 615-620.
HOWARD, C. J., BALL, C. J., DAVIS, L. D. & ELCOMBE, M. M. (1983). *Aust. J. Phys.* **35**, 507-518.
KESSON, S. (1983). *Radioact. Waste Manage.* **4**, 53-72.
KESSON, S. & WHITE, T. J. (1986). *Proc. R. Soc. London Ser. A.* In the press.
POST, J. E., VON DREELE, R. B. & BUSECK, P. R. (1982). *Acta Cryst.* B**38**, 1056-1065.
PRING, A. (1983). PhD Thesis, Univ. of Cambridge.
RIETVELD, H. M. (1969). *J. Appl. Cryst.* **2**, 65-71.
RINGWOOD, A. E. (1978). *Safe Disposal of High Level Radioactive Waste: A New Strategy.* Canberra: Australian National University Press.
ROTH, R. (1981). Annual Report. National Measurement Laboratory, Office for Nuclear Technology. NBSIR 81-2241.
SABINE, T. M. & HEWAT, A. W. (1982). *J. Nucl. Mater.* **110**, 173-177.
SHANNON, R. D. (1976). *Acta Cryst.* A**32**, 751-767.
SINCLAIR, W., MCLAUGHLIN, G. M. & RINGWOOD, A. E. (1980). *Acta Cryst.* B**36**, 2913-2918.
SOLOMAH, A. G. & ODOJ, R. (1984). *J. Am. Ceram. Soc.* **67**, C-50-C-51.
WEBER, H. & SCHULZ, H. (1983). *Solid State Ionics*, **9** & **10**, 1337-1340.
WILES, D. B. & YOUNG, R. A. (1981). *J. Appl. Cryst.* **14**, 149-150.

Acta Cryst. (1987). B**43**, 34-40

$Mg_7Ga_2GeO_{12}$, a New Spinelloid-Related Compound, and the Structural Relations Between Spinelloids (Including Spinel) and the β-Ga_2O_3 and NaCl Types

BY J. BARBIER

Department of Geology, University of Western Ontario, London, Ontario N6A 5B7, Canada

AND B. G. HYDE

Research School of Chemistry, Australian National University, GPO Box 4, Canberra-ACT 2601, Australia

(*Received* 25 *April* 1986; *accepted* 13 *July* 1986)

Abstract

A new compound, $Mg_7Ga_2GeO_{12}$, has been identified in the MgO–Ga_2O_3–GeO_2 system (at 1 atmosphere pressure). Its unit cell is orthorhombic with parameters $a = 5{\cdot}8493\,(5)$, $b = 25{\cdot}449\,(3)$ and $c = 2{\cdot}9816\,(3)$ Å, with $V = 443{\cdot}8$ Å^3, $Z = 2$, $D_x = 4{\cdot}30$ g cm^{-3} and $M_r = 574{\cdot}2$. A structural model, determined from powder X-ray diffraction data, shows that it is isostructural with Fe_9PO_{12}. Its crystal structure is simply related to that of the spinelloid phases and, like them, can be described as an intergrowth of the rock salt and β-Ga_2O_3 types.

1. Introduction

We recently reported the identification of a new compound, $Mg_3Ga_2GeO_8$(III) (Barbier & Hyde, 1986), stable at atmospheric pressure in the MgO–Ga_2O_3–GeO_2 system and isostructural with the spinelloid β-phase [*e.g.* β-Co_2SiO_4 (Morimoto, Tokonami, Watanabe & Koto, 1974) and $Ni_3Al_2SiO_8$(III) (Ma & Sahl, 1975)]. $Mg_3Ga_2GeO_8$(III) was the first (pseudo)ternary phase identified in that system, while the previously known (pseudo)binary phases – in the magnesium-rich region of the phase diagram – included $MgGa_2O_4$ spinel (*e.g.* Schmalzried, 1961),

0108-7681/87/010034-07$01.50